Semicond. Sci. Technol. **24** (2009) 105028 (5pp) doi:10.1088/0268-1242/24/10/105028

Effect of the plasma composition on the structural and electronic properties of as-grown SiO_x/Si heterolayers deposited by reactive sputtering

E Mota-Pineda[1,2], M Meléndez-Lira[3,6], M Zapata-Torres[3], A Pérez-Centeno[4], M A Santana-Aranda[4] and P del Angel[5]

[1] Departamento de Física, Cinvestav IPN, Apdo. 17-740 México DF, México 07000, Mexico
[2] Academia de Matemáticas, ESIME ZAC, Unidad profesional Adolfo López Mateos, 07738 DF, Mexico
[3] CICATA-IPN, Unidad Legaria, Legaria 694 Col. Irrigación, Del. Miguel Hidalgo, C.P. 11500, Mexico DF, Mexico
[4] Departamento de Física, CUCEI, Universidad de Guadalajara, Blvd. Marcelino García Barragán # 1421, Col. Olímpica, CP, 44430, Guadalajara, Jal., Mexico
[5] Instituto Mexicano del Petróleo, Dirección de Investigación y Posgrado, Eje Central L. Cárdenas 152, 07730 México, DF, Mexico

E-mail: emota@fis.cinvestav.mx

Received 25 April 2009, in final form 22 July 2009
Published 25 September 2009
Online at stacks.iop.org/SST/24/105028

Abstract
We report the effects of varying the oxygen partial pressure (OPP) on the structural and electronic properties of SiO_x/Si heterolayers grown by RF reactive sputtering. The produced samples present silicon poly-crystalline characteristics for low values of OPP. The crystallinity decreases as the OPP increases due to oxygen interdiffusion until the silicon crystal structure becomes amorphous. The results of infrared and Raman spectroscopies show higher deviation from stoichiometry and an increment of structural disorder for samples grown with higher values of OPP. Room temperature photoluminescence (PL) is present in all as-grown samples. The PL spectra show two bands, around 1.87 and 2.16 eV, for all the samples, while a third broad band at lower energy shows up and shifts to the red as OPP increases. Our results indicate that silicon-related room temperature PL emission is correlated with the stoichiometry of the SiO_x and to the formation of silicon crystals embedded in a silicon dioxide matrix.

1. Introduction

Silicon, the dominant material in the electronic industry, has an indirect band gap which limits its efficiency as a light emitter. This fact has precluded the achievement of silicon-based optoelectronic systems for a long time. Over the last few years, several works have shown that it is possible to obtain light emission from silicon-based materials by doping with rare earth elements [1, 2], low-dimensional [3, 4] and stressed systems [5]. Another approach is through the synthesis of non-stoichiometric silicon dioxide [6–9]. These studies have been done employing almost all of the growth techniques available to materials science. Even when the mechanisms of the photoluminescence emission still are under discussion, it is desirable to have reliable methods to produce light emission in silicon-based materials in order to strengthen its application in opto-electronic devices [10–12]. In this paper, we present the results of the structural and electronic properties of a set of SiO_x/Si/SiO_x heterostructures grown by reactive sputtering on silicon substrates. The samples were grown from a silicon target, varying the oxygen partial pressure (OPP) employed for the deposition of silicon oxide layers. The inclusion of the silicon interlayer along with the oxygen interdiffusion process that takes place during the deposition promotes that the SiO_x/Si/SiO_x heterostructures exhibit a strong dependence of its structural and electronic

[6] On sabbatical leave from Departamento de Física, Cinvestav-IPN.

 © 2009 IOP Publishing Ltd Printed in the UK

properties on the OPP values. The overall characteristics of the heterostructures can be described in an effective way through the stoichiometry of a silicon dioxide layer with silicon inclusions. A decrease in silicon crystallinity, an increase in non-stoichiometric characteristics of the SiO_x and a broader room temperature (RT) photoluminescence (PL) emission are obtained for the samples as the OPP values augment. The modification of the stoichiometry of the SiO_x layers and the growth of silicon crystallites embedded in a silicon dioxide matrix through the oxidation of the silicon interlayer give place to a broad RT PL emission from 1.4 eV up to 2.2 eV.

2. Experimental details

A set of $SiO_x/Si/SiO_x$ heterolayers were synthesized employing a radio frequency magnetron sputtering system. The samples were grown from a polycrystalline silicon target on Czochralski-grown Si(1 0 0) substrates heated at 400 °C. The silicon oxide films were grown by reactive sputtering of the silicon target employing a plasma mixture of oxygen (O_2) and argon (Ar), whereas the Si layer was deposited cutting off the oxygen flow. The total gas pressure in the chamber was kept constant at 15 mTorr during the deposition of the heterostructure. After the deposition of each layer the plasma was turned off and the chamber was evacuated to 10^{-7} Torr, then the OPP growth condition was recovered. The OPP was determined with respect to the total gas pressure. The RF power applied to the target was 200 W. We prepared five samples employing different OPP to grow the silicon oxide layers: 25% (sample OPP25), 33% (sample OPP33), 50% (sample OPP50), 66% (sample OPP66) and 75% (sample OPP75). The thickness of the layers was controlled by the deposition time: 25 min for the deposition of each silicon oxide layer and 10 min for the Si layer. When the growth was finished, the samples were maintained inside the system until room temperature was attained. As reference samples, a set of silicon dioxide films were deposited for 60 min under the same OPP conditions employed to grow the heterostructures; the thickness of these samples was around 300 nm.

The layer structure of the samples was observed by cross-section transmission electron microscopy (TEM), using a JEOL2010 system operated at 200 kV; the sample preparation was performed by typical lapping, polishing and PIPS (precision ion polishing system), whereas the images were recorded by a charge-coupled device. The crystallographic properties of the samples were studied by grazing incidence x-ray diffraction carried out in a Siemens D5000 system employing the Cu K_α wavelength. The infrared (IR) transmission spectra were obtained employing a Nicolet 750 FTIR system. Micro-Raman spectroscopy was carried out in a Horiba Jobin Yvon LabRAM system employing the 488 nm line of an Ar+ ion laser as an excitation source, in a backscattering cross polarized configuration. The power density of the laser was 200 W cm^{-2}, and there was no evidence of changes in the properties of the samples due to laser intensity. PL measurements were carried out employing a lock-in standard technique using a 275 M Acton single spectrometer equipped with a 1200 lines/mm grating blazed at 500 nm and a GaAs(Cs) Hamamatsu photomultiplier as a detector; the width of both slits was set at 50 μm. The excitation source was a 473.8 nm diode pumped solid-state laser.

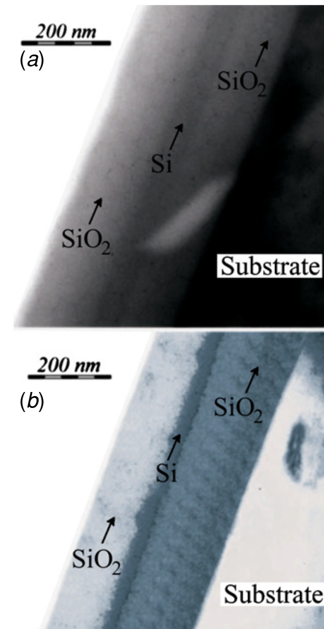

Figure 1. Cross-section TEM micrographs of the heterostructures. (*a*) OPP25 and (*b*) OPP75.

3. Results and discussion

Besides the effect on surface topography, the change in OPP has no influence on the structural and electronic characteristics of reference samples [13]. Infrared spectroscopy and x-ray diffraction results indicated that all silicon dioxide reference samples presented the stoichiometry of SiO_2 with an amorphous structure independently of the OPP employed. The presence of silicon particles embedded within the reference films was discarded by the Raman spectroscopy results and accordingly PL emission was absent.

Representative cross-section TEM micrographs are presented in figure 1: (*a*) OPP25 and (*b*) OPP75. These images show clearly the different layers of the $SiO_x/Si/SiO_x/Si$-substrate heterostructure. The heterostructure thicknesses are similar independently of growth conditions, see table 1. However, the silicon interlayer presents features depending on the OPP employed to grow the silicon oxide layer. Although deposition conditions for the silicon interlayer are the same for the whole set of samples, for sample OPP25 (figure 1(*a*)) a thicker layer with smoother interfaces is clearly observed as compared with that shown for sample OPP75 (figure 1(*b*)). As OPP is increased a greater amount of oxygen is available to react with the silicon interlayer giving place to the formation of silicon dioxide rich in silicon. Due to the gradual oxidation of the silicon interlayer, when the deposition of the top layer of SiO_2 stops, in the interface SiO_x/Si, there remain some clusters of silicon embedded in SiO_x. The above-mentioned fact produce a rougher SiO_x/Si interface and a decrease in the

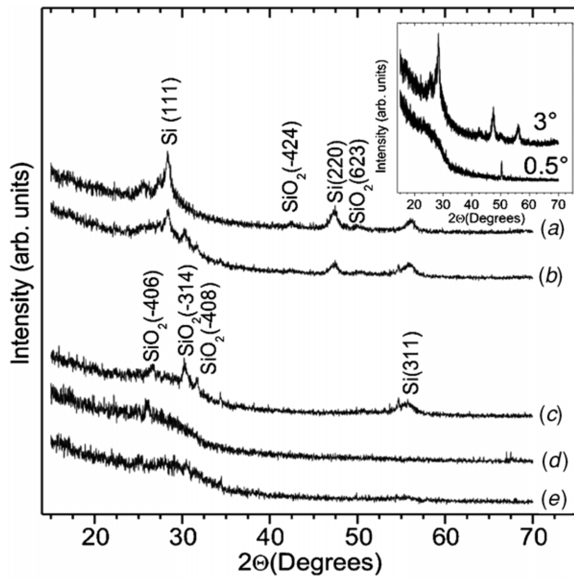

Figure 2. GIXRD patterns of the samples obtained employing a grazing angle of 3°. (*a*) OPP25, (*b*) OPP33, (*c*) OPP50, (*d*) OPP66 and (*e*) OPP75. In the inset, GIXRD patterns of the sample OPP25 obtained employing a grazing angle of 0.5° and 3°.

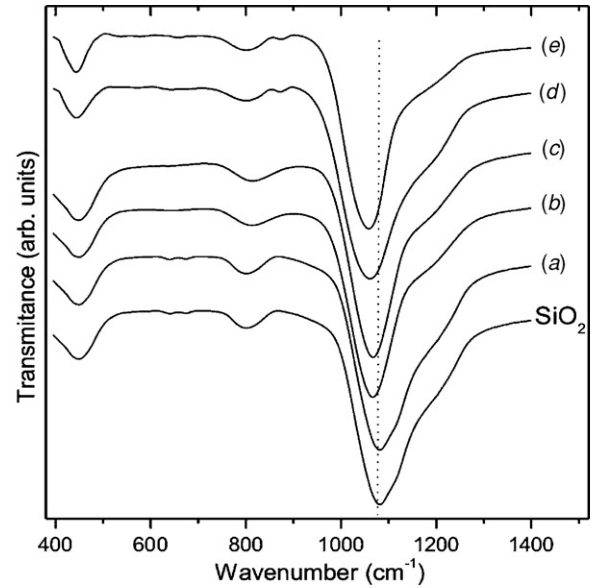

Figure 3. FTIR spectra of the studied samples. The spectrum with the SiO_2 label corresponds to a reference sample. (*a*) OPP25, (*b*) OPP33, (*c*) OPP50, (*d*) OPP66 and (*e*) OPP75. The dot line is a guide to the eye.

Table 1. Thicknesses of the heterostructures and frequency of the IR stretching peak and *x*-value obtained for the effective SiO_x composition [14].

Sample	Thickness (nm)	Frequency (cm^{-1})	x
OPP25	350	1080	2.00
OPP33	340	1070	1.85
OPP50	330	1065	1.78
OPP66	325	1060	1.71
OPP75	320	1056	1.64

thickness of the silicon interlayer as can be observed for the sample growth employing the higher OPP, see figure 1(*b*).

X-ray diffractograms (XRD), with a grazing incidence angle of 3°, of the $SiO_x/Si/SiO_x$ heterostructures are shown in figure 2. The peaks were indexed using the powder diffraction files 271 402 for cubic silicon and 181 178 for monoclinic SiO_2. In the XRD shown in figures 2(*a*) and (*b*) (OPP25 and OPP33), we can observe the peak corresponding to the (1 1 1) plane of cubic silicon and peaks related to the SiO_2. Sample OPP50 also presents a mixture of phases but with a diminished proportion of crystalline silicon, figure 2(*c*). On the XRD shown in figures 2(*d*) and (*e*), we only have peaks related to SiO_2 and a broad feature due to amorphous silicon. In order to determine the origin of the crystalline reflections, we measured the sample with the higher crystallinity (OPP25) at a grazing angle of 0.5°. In the inset shown in figure 2 are included both 0.5° and 3.0° grazing angle XRD; we can observe that the XRD for 0.5° (lower diffractogram) presented an amorphous characteristic, and we have only one peak related to the SiO_2 phase, plane (623). These suggest that the crystalline reflections are due to the silicon interlayer of the heteroestructure while the SiO_x layers are amorphous, in agreement with the results of the reference samples. The presence of diffraction peaks from SiO_2 crystallographic planes indicates the growth of SiO_2 crystals which are formed at the silicon interlayer during the sputtering process. The crystallinity of the silicon interlayer decreases with the increase of OPP due to a higher interaction with oxygen.

Figure 3 shows the IR transmission spectra obtained for the $SiO_x/Si/SiO_x$ heterostructures, including the spectrum from a SiO_2 sample as reference. The IR bands related to stretching, bending and rocking vibrational modes of Si–O–Si bonds for stoichiometric SiO_2 samples are located at 1080, 812 and 458 cm^{-1}, respectively. The dotted line shown in figure 3 allows us to follow the shift in the band around 1080 cm^{-1}. The shift toward lower energies of the IR bands is associated with the formation of sub-oxide phases and is widely employed to evaluate the stoichiometry of silicon oxide. We considered the relation $x = (\upsilon - 940)/70$ between the frequency of the band υ and the oxygen content x [14]; the values obtained are presented in table 1. In our case, it is clear that the IR signal comes from the whole heterostructure, but it allows us to estimate the stoichiometry of the silicon-rich region which corresponds to the silicon interlayer. These results indicate that the oxidation process of the silicon interlayer increases for the higher values of OPP employed, supporting our interpretation of TEM micrographs and x-ray diffraction results.

The Raman spectra of the studied samples are shown in figure 4. In spite of the fact that all samples were deposited under similar conditions, the characteristic Raman peak at 521 cm^{-1} associated with the silicon substrate increases its strength as the OPP value increases, see figures 4(*a*)–(*e*).

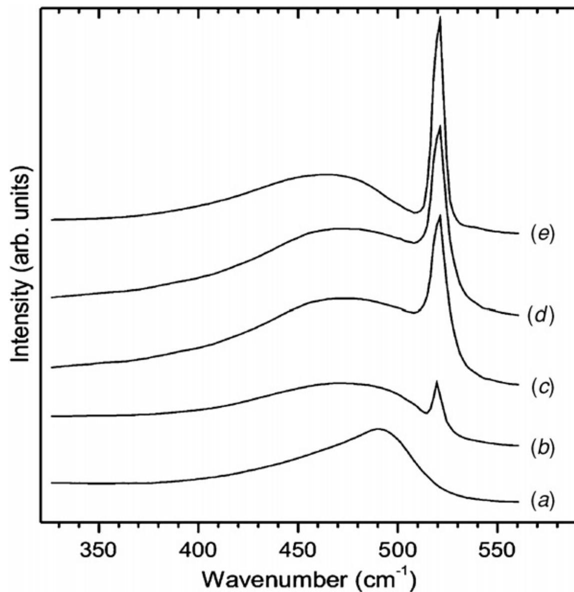

Figure 4. Raman spectra of the samples: (*a*) OPP25 (*b*) OPP33, (*c*) OPP50, (*d*) OPP66 and (*e*) OPP75.

This fact is associated with a greater transparency to the excitation laser energy of the $SiO_x/Si/SiO_x$ heterostructures, as the process of oxidation of the silicon interlayer increases due to the increment of the OPP. Also it should be noted that the silicon substrate signal is superimposed onto broader signals coming from the $SiO_x/Si/SiO_x$ heterostructures. Raman spectra features agree with the results of x-ray diffraction: as OPP increases the silicon Raman signal from the $SiO_x/Si/SiO_x$ heterostructures becomes broader with its maximum shift toward lower energies indicating an increasing silicon structural disorder. The broad band around 490 cm^{-1} in the Raman spectrum reported in figure 4(*a*) can be described as due to the superposition of signals coming from (i) silicon nanoparticles, (ii) partially crystallized silicon and (iii) amorphous silicon [15]. For the whole set of samples, all the above-mentioned contributions are present at different extent and are reflected in the redshift of the broad Raman peak, see figures 4(*a*)–(*e*). For the sample grown with the highest OPP, the signal comes mainly from the SiO_x in agreement with IR spectroscopy results.

A relevant characteristic of the approach employed in this work to grow the heterolayers is that all the samples showed PL emission without additional thermal treatment. Figure 5 shows the RT PL spectra for the whole set of samples. The PL spectra were corrected for the spectral sensitivity of the system, taking in account the characteristics of the grating and the detector employed.

The photoluminescence emission is broad, depending on the preparation conditions. For all the PL spectra, we identify the presence of two bands at 1.87 and 2.16 eV and for samples grown at OPP >25%, a third low-energy band is present; as OPP increases its peak energy shifts to lower energies and its strength increases. The dashed line curves shown in figure 5 correspond to the three Gaussian curves employed to fit the experimental PL spectra; table 2 shows the fitting values.

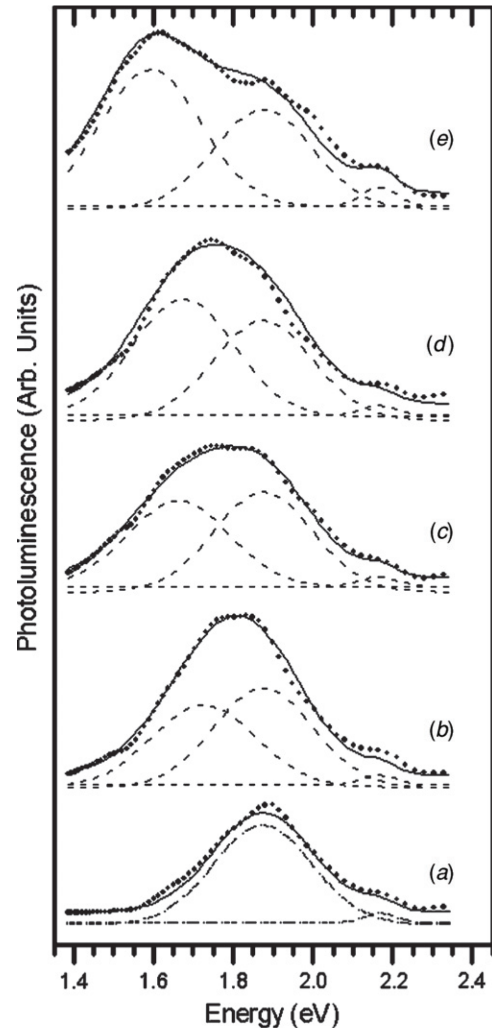

Figure 5. Room temperature photoluminescence spectra for the heterostructures. (*a*) OPP25, (*b*) OPP33, (*c*) OPP50, (*d*) OPP66 and (*e*) OPP75. The continuous line represents the fitting to the experimental PL spectrum shown as dots. The broken line represents each Gaussian contribution.

The constant value of the high-energy bands, independently of the OPP employed, suggests that there is a common mechanism for the photoluminescence emission. The details of preparation of the $SiO_x/Si/SiO_x$ heterostructures allow us to establish the origin of the PL emission as a superposition of silicon-rich oxide and quantum confinement effects in silicon clusters embedded in a silicon-rich oxide matrix. The x-ray and IR spectroscopy characterization clearly indicate that disorder and deviation from the stoichiometry composition of SiO_2 increase for greater OPP values. Then, the origin of the low-energy band could be associated with the presence of a silicon-rich silicon dioxide while that of the higher energy bands could be due to quantum confinement in silicon clusters [16]. The mass effective model of quantum confinement [17] indicates that high-energy peaks are due to nanoparticles with mean diameters of 3.7 nm and 3.4 nm indicating that the particle size is self-regulated by the growth process. A detailed study of PL emission will be presented elsewhere.

Table 2. Energy and full width at half maximum (FWHM) of the three Gaussian curves employed for fitting the PL spectra of the heterostructures.

Sample	Gaussian A		Gaussian B		Gaussian C	
	Energy (eV)	FWHM (eV)	Energy (eV)	FWHM (eV)	Energy (eV)	FWHM (eV)
OPP25	2.16	0.11	1.87	0.31	–	–
OPP33	2.16	0.11	1.87	0.31	1.72	0.33
OPP50	2.16	0.11	1.87	0.31	1.67	0.31
OPP66	2.16	0.11	1.87	0.31	1.65	0.30
OPP75	2.16	0.11	1.87	0.31	1.59	0.32

4. Conclusions

The growth of $SiO_x/Si/SiO_x$ heterostructures by RF reactive sputtering is a direct method to obtain room temperature photoluminescence emission from as-grown silicon-based materials. As OPP increases the crystallinity of Si interlayer decreases until it becomes totally amorphous. The $SiO_x/Si/SiO_x$ heterostructures can be described considering an effective SiO_x layer; when OPP increases its non-stoichiometry also increases. The spectral distribution of the photoluminescence emission has its origin in the quantum confinement in silicon nanocrystals and in mechanisms associated with the presence of non-stoichiometric silicon oxide regions. Lower OPP values favor the synthesis of smoother silicon/dielectric interfaces and PL emission due mainly to quantum confinement in silicon clusters. Size distribution of silicon particles is self-regulated by the growth process. As OPP increases a broad PL band originated from the presence of non-stoichiometric silicon oxide emerges. The approach reported here allows us to control the spectral distribution of PL through the stoichiometry of the silicon dioxide without any additional process besides the modification of the preparation conditions of the silicon oxide layer.

Acknowledgments

The technical support of M Guerrero, A Garcia-Sotelo and E Gomez is greatly acknowledged. This work was partially supported by CONACyT-Mexico. We acknowledge the fruitful discussions with A Zapata-Navarro.

References

[1] Rozo C, Fonseca L F, Jaque D and Sole J G 2008 *J. Lumin.* **128** 897
[2] Rinnert H, Adeola G W and Vergnat M 2009 *J. Appl. Phys.* **105** 036101
[3] Ren F F, Yu M B, Ye J D, Chen Q, Tan S T, Lo G Q and Kwong D L 2008 *J. Appl. Phys.* **93** 091901
[4] Cho E U, Green M A, Corkish R, Reece P, Gal M and Lee S H 2007 *J. Appl. Phys.* **101** 024321
[5] Ahmad I, Temple M P, Kallis A, Wojdak M, Oton C J, Barbier D, Saleh H, Kenyon A J and Loh W H 2008 *J. Appl. Phys.* **104** 123108
[6] Podhorodecki A, Misiewicz J, Gourbilleau F and Rizk R 2008 *Electrochem. Solid-State Lett.* **11** K31
[7] Pan W, Dunn R G, Carroll M S, Banks J C and Brewer L N 2008 *J. Non-Cryst. Solids* **354** 975
[8] Silalahi S T H, Yang H Y, Pita K and Mingbin Y 2009 *Electrochem. Solid-State Lett.* **12** K29
[9] Flores F, Aceves M, Carrillo J, Domínguez C and Falcony C 2005 *Superficies y Vacío* **18** 7
[10] Cazzanelli M, Navarro-Urrios D, Riboli F, Daldosso N, Pavesi L, Heitmann J, Yi L X, Scholz R, Zacharias M and Gosele U 2004 *J. Appl. Phys.* **96** 3164
[11] Pavesi L, DalNegro L, Mazzoleni C, Franzo G and Priolo F 2000 *Nature* **408** 440
[12] Hao X J, Cho E C, Flynn C, Shen Y S, Park S C, Conibeer G and Green M A 2009 *Sol. Energy Mater. Sol. Cells* **93** 273
[13] Mota-Pineda E and Meléndez-Lira M 2008 *J. Appl. Phys.* **104** 064316
[14] Jambois O, Rinnert H, Devaux X and Vergnat M 2006 *J. Appl. Phys.* **100** 123504
[15] Fauchet P M and Campbell I H 1988 *Crit. Rev. Solid State Mater. Sci.* **14** S79 See for instance and references therein
[16] Iacona F, Franzo G and Spinella C 2000 *J. Appl. Phys.* **87** 1295 See for instance and references therein
[17] Nae-Man P, Chel-Jong C, Seong T Y and Park S J 2001 *Phys. Rev. Lett.* **86** 1355